Naval Research Laboratory

Washington, DC 20375-5320

NRL/MR/7130--97-7974

Comparison Between the Tap Model and Sara-2d Results

ANGIE SARKISSIAN

Physical Acoustics Branch
Acoustics Division

September 12, 1997

REPORT DOCUMENTATION PAGE

Form Approved
OMB No. 0704-0188

1. AGENCY USE ONLY (*Leave Blank*)	2. REPORT DATE	3. REPORT TYPE AND DATES COVERED
	September 12, 1997	Interim Report

4. TITLE AND SUBTITLE

Comparison Between the Tap Model and Sara-2d Results

5. FUNDING NUMBERS

6. AUTHOR(S)

Angie Sarkissian

7. PERFORMING ORGANIZATION NAME(S) AND ADDRESS(ES)

Naval Research Laboratory
Washington, DC 20375-5320

8. PERFORMING ORGANIZATION REPORT NUMBER

NRL/MR/7130--97-7974

9. SPONSORING/MONITORING AGENCY NAME(S) AND ADDRESS(ES)

Office of Naval Research
Arlington, VA 22217-5000

10. SPONSORING/MONITORING AGENCY REPORT NUMBER

11. SUPPLEMENTARY NOTES

12a. DISTRIBUTION/AVAILABILITY STATEMENT

Approved for public release; distribution unlimited.

12b. DISTRIBUTION CODE

13. ABSTRACT (*Maximum 200 words*)

The Technical Advisory Panel (TAP) has developed a simple model for the bistatic response of a submarine consisting of four scattering mechanisms: the backscattering response from a finite cylinder, forward scattering from a finite cylinder, scattering from hemispherical end-caps and scattering of elastic waves in the cylinder. Scattering results using the tap model are compared to computations made using finite elements/infinite elements method for a finite cylindrical shell with hemispherical end-caps for two different cases. In the first case the cylinder does not contain ribs. In the second case the cylinder contains eighty-five ribs with equal spacing between any two adjacent ribs. Comparisons show that major scattering features such as a strong specular reflection or the strong forward scattering field look similar using the two approaches but differences can be observed between the two results. The tap model predicts a lower forward scattered field at some angles, specially near end incidence.

14. SUBJECT TERMS

Acoustic scattering
Target strength

15. NUMBER OF PAGES

13

16. PRICE CODE

17. SECURITY CLASSIFICATION OF REPORT	18. SECURITY CLASSIFICATION OF THIS PAGE	19. SECURITY CLASSIFICATION OF ABSTRACT	20. LIMITATION OF ABSTRACT
UNCLASSIFIED	UNCLASSIFIED	UNCLASSIFIED	UL

NSN 7540-01-280-5500

Standard Form 298 (Rev. 2-89)
Prescribed by ANSI Std 239-18
298-102

COMPARISON BETWEEN THE TAP MODEL AND SARA-2D RESULTS

I. Introduction

The Technical Advisory Panel (TAP), sponsored by N87, ARPA and PD80 has recently provided a simple model for the bistatic target strength of submarines[1]. The members of the TAP working group for target strength are: Dr. Harry Cox, Dr. Nolan Davis, Dr. John Hanna and Dr. Kevin McCann. The model they have provided contains four scattering mechanisms: (1) backscattering from a finite cylinder, (2) forward scattering from a finite cylinder, (3) scattering from hemispherical end-caps and (4) scattering of elastic waves in the cylinder. In this article, the results of the TAP model are compared to scattering from a finite cylindrical shell with hemispherical end-caps computed using program Sara-2d[2] which uses finite elements to model the cylindrical structure and finite and infinite elements to model the unbounded fluid medium outside the structure. For additional details on the finite and infinite elements method, the reader is referred to Ref [3,4]. Next, since submarines contain ribs with periodic spacing, the results of the TAP model are compared to scattering from the same cylindrical shell but containing eighty-five ribs with equal spacing between adjacent ribs. The scattering computations are made using Sara-2d again. The periodicity of the ribs introduces Bloch Wave resonances and Bragg scattering peaks that are not included in the TAP model.

II. The TAP Model

Figure 1 shows the geometry used. The target is a finite cylinder with hemispherical end-caps having length L and radius a. The figure shows the source angle θ_S and the receiver angle θ_R. For the backscattering contribution to the acoustic intensity, the TAP model uses

$$\sigma_1 = \frac{aL^2}{\lambda} \frac{\sin\theta_S \sin\theta_R}{(\sin\theta_S + \sin\theta_R)} j_o^2(kL\cos\theta_E), \tag{1}$$

where

$$\cos\theta_E = \frac{\cos\theta_S + \cos\theta_R}{2},$$

λ is the wavelength and k is the wavenumber of the acoustic field.

For the contribution to acoustic intensity resulting from end-caps, the TAP model uses

$$\sigma_2 = \begin{cases} \frac{1}{2}\left[.69(ka)^4 \frac{a^2}{4}\right], & \text{if } ka \le 1.1 \\ \frac{1}{2}\frac{a^2}{4}, & \text{if } ka > 1.1 \end{cases} \tag{2}$$

Manuscript approved August 4, 1997

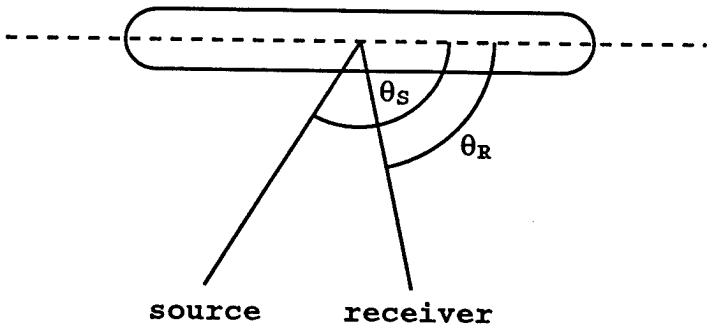

FIG. 1. Geometry showing source angle θ_S and receiver angle θ_R.

This intensity is half as large as the intensity resulting from the end-cap of a hemispherically end-capped cylinder. The factor of $\frac{1}{2}$ is present because submarines tend to be tapered cylinders and thus have a smaller effective hemispherical radius.

TAP uses a modified version of Babinet's Principle[5] for the contribution of the acoustic intensity from forward scattering. The version that is used imposes reciprocity and is given by

$$\sigma_3 = \left(\frac{2aL}{\lambda}\right)^2 |\sin\theta_S \sin\theta_R| j_o^2(kL\cos\theta_E). \tag{3}$$

Finally, TAP models the contribution of the elastic waves to the acoustic intensity by

$$\sigma_4 = P(\theta_S)P(\theta_R), \tag{4}$$

where

$$P(\theta) = \begin{cases} \frac{BL}{\pi}\cos\left[\frac{\pi}{2\alpha}\frac{\hat{\theta}}{\left(\frac{\pi}{2}-\theta_{lim}\right)}\right], & \text{if } |\hat{\theta}| < \alpha|\frac{\pi}{2}-\theta_{lim}| \\ 0, & \text{if } |\hat{\theta}| \geq \alpha|\frac{\pi}{2}-\theta_{lim}| \end{cases}, \tag{5}$$

$$\hat{\theta} = |\theta - \pi| - \frac{\pi}{2},$$

$$\cos\theta_{lim} = \frac{c}{c_v},$$

c is the speed of sound in the acoustic medium and c_v is the compressional or the sheer speed in the shell, α is a scaling factor having a typical value of 2 and B is an efficiency factor having a typical value of 0.2.

III. Comparisons

Results computed using the TAP model are compared to scattering computations made for the cylinder shown in figure 2. The cylinder has a radius $a = 3.09m$, length $L = 42.3m$ and thickness $t = .023m$. It contains eighty-five ribs of two different lengths. The short ribs have a length of $.24m$ and a thickness of $.020m$. Every thirteenth rib is longer having a length of $.43m$ and a thickness of $.023m$. The elastic parameters used are that of nickel with modulus of elasticity of $2.1 \times 10^{11} Pa$, Poisson's ratio of .30 and density of $8800 kg/m^3$ which results in a compressional sound speed of $5670 m/s$ and a shear sound speed of $3030 m/s$. The exterior acoustic field has sound speed of $1510 m/s$ and density of $1000 kg/m^3$.

FIG. 2. The ribbed finite cylinder used for the computations..

Figure 3 shows target strength results using the TAP model compared to Sara-2d computations for a cylinder that does not contain any ribs. Results are shown as a function of source angle and receiver angle at a frequency of $299 Hz$ or $ka = 3.84$. The two plots show similar major features. Both plots show a strong specular reflection, the red highlight at the lower part of the plots, and a strong forward field, the red highlight at the upper part of the plots. Yet some differences can be observed between the two plots. For example the elastic wave contributions appear as rectangular highlights around the specular and forward returns in the TAP model predictions but they are concentrated at specific narrower regions in the Sara-2d results. We also observe a stronger forward scattering response in the Sara-2d results specially near source angles of 90° and 180°. Additionally, the specular return, computed using the Sara-2d results contains some minima produced by the interference of the elastic waves with the reflected wave. At a source angle of 180° and a receiver angle of 180°, which is the end-incident backscattering condition, a highlight is observed in the Sara-2d results which is not present in the TAP model.

Figure 4 shows bistatic plots of target strength of the same cylinder for a source angle of 75° and frequency ranging between $200 Hz$ and $500 Hz$. Again a strong specular return can be observed at 105° and a strong forward field at 255° in both plots. Although the major features are similar in the two plots, some differences can be observed. The elastic wave is modeled as a cosine functions centered at 90° and 270° in the TAP model yet it has different shape in the Sara-2d results.

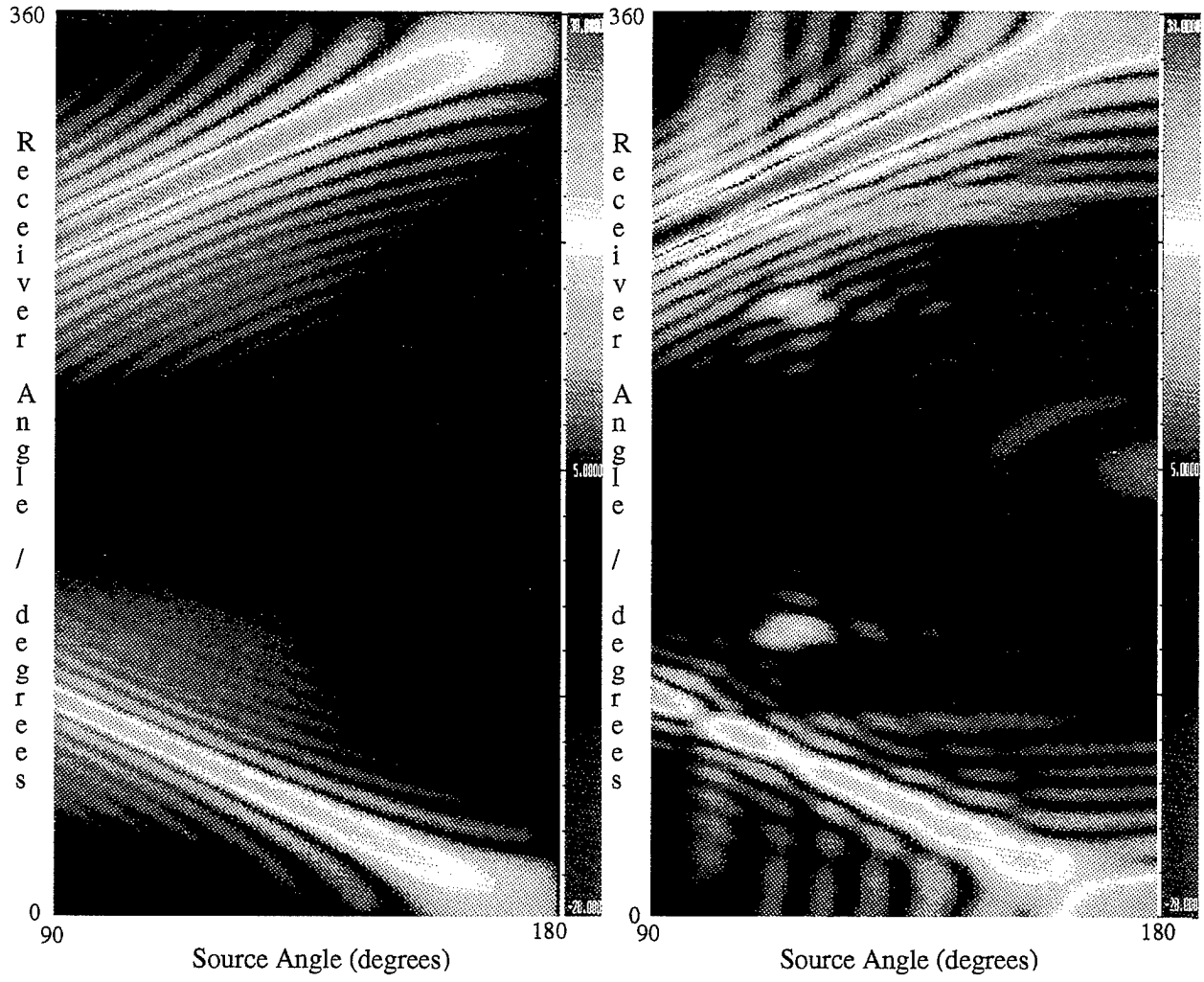

FIG. 3. Target strength at a frequency of 299Hz, ka=3.84, using (a) the TAP model and (b) Sara–2d computations.

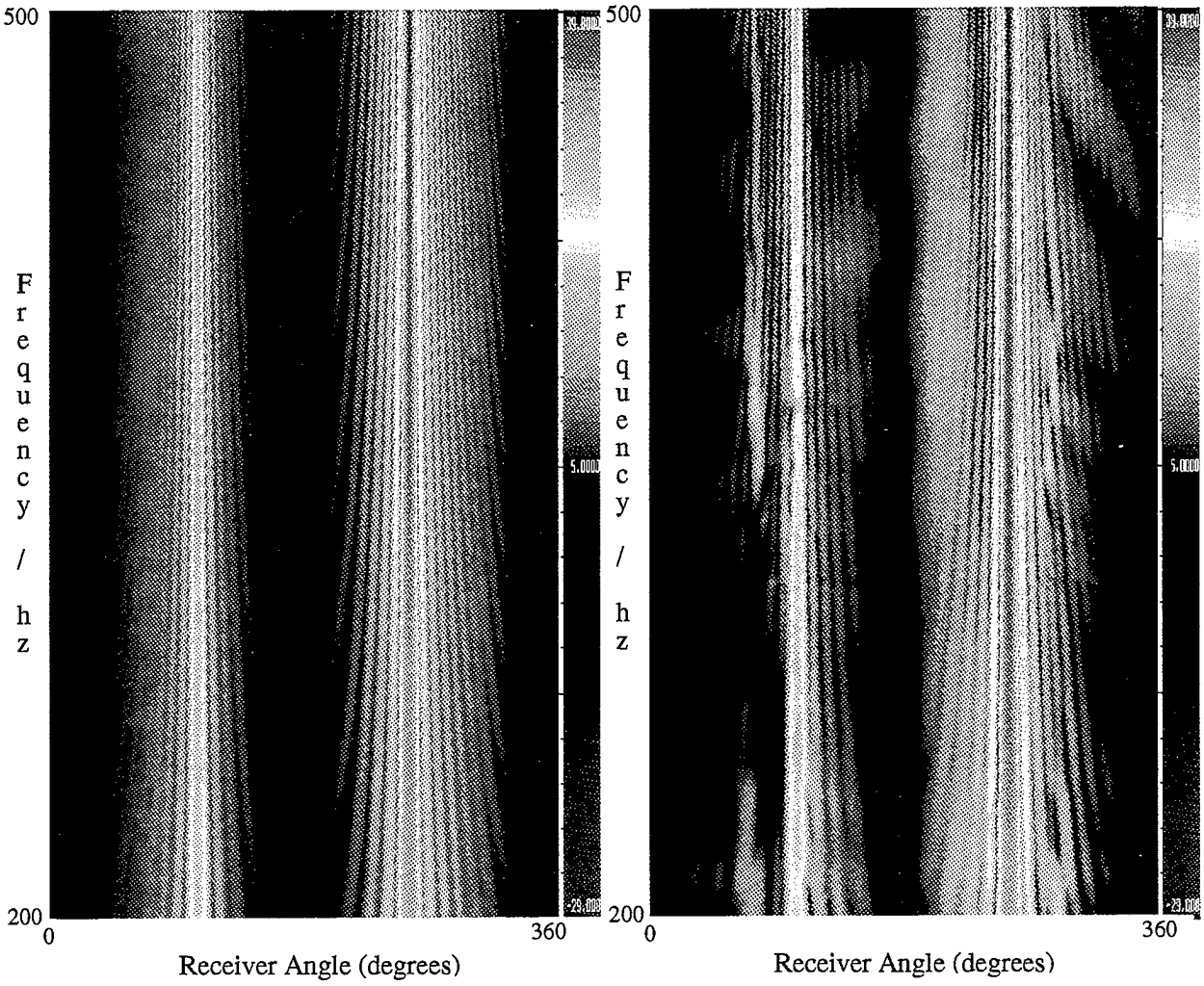

FIG. 4. Bistatic target strength for a source angle of 75 degrees using (a) the TAP model and (b) Sara–2d computations.

Figure 5 shows monostatic plots for the same cylinder using the two methods of computation again where an angle of 0° represents end incidence backscattering and an angle of 90° represents normal incidence. Both plots contain a strong specular return at an angle of 90° but the Sara-2d results show a minimum at a frequency of $260Hz$ which is not present in the TAP model. The minimum is produced by the elastic wave that travels circumferentially along the cylinder and interferes with the specular. The additional elastic wave contribution is different in the two plots. It has the shape of a cosine function in the TAP model producing enhanced target strength in a rectangular region to the right of the figure while it is confined to certain frequency/angle regions in the Sara-2d results.

Computations are next made using a ribbed cylinder as the target. Figure 6 shows target strength results as a function of source angle and receiver angle at a frequency of $700Hz$ or $ka = 9.00$, where Bloch waves are present. Again, although the major features such as the specular return and forward scattering are similar in the two plots, some differences can be observed. The forward scattered field is lower in the TAP model specially near end incidence at source angle of 180° and a receiver angle of 360°. Other differences are present in the way the supersonic elastic wave contributions are modeled in the TAP results and the neglect of the Bloch wave resonances in the model.

Figure 7 shows bistatic target strength results for the ribbed cylinder for a source angle of 80° and frequency ranging between $200Hz$ and $1.5kHz$. The strongest highlights in the two plots are the specular return at an angle of 100° and the forward field at an angle of 260° but, again, differences can be observed between the two plots.

Figure 8 shows monostatic plots of target strength values for the ribbed cylinder for frequency ranging between $200Hz$ and $2kHz$. Both plots show a strong specular field at 90° but Sara-2d computations show Bloch wave resonances which are the highlights between $600Hz$ and $800Hz$ and between $1kHz$ and $1.6kHz$ and Bragg diffraction above $1.7kHz$ which are not present in the TAP model. Additionally the contribution of the supersonic elastic waves produce highlights in the monostatic response that are confined to certain regions in frequency/angle plot of the Sara-2d results that appear different from the TAP model.

IV. Conclusion

Comparisons between the TAP model and Sara-2d computations show that the major features such as the specular reflection and the strong forward scattering predictions are similar using the two computational techniques but differences can be observed between the results computed using the two methods. The forward scattered field predicted by the TAP model is lower near end incidence. Other differences are present in the way the elastic wave contribution is modeled in the TAP model and, in case of a ribbed cylindrical shell, the TAP model does not include any Bloch wave resonances or Bragg scattering peaks both of which are produced by the periodicity of the rib spacing.

[1]John S. Hanna, "Implications of a Bistatic Target Strength Model," SAIC Report 96/1045 (1996).

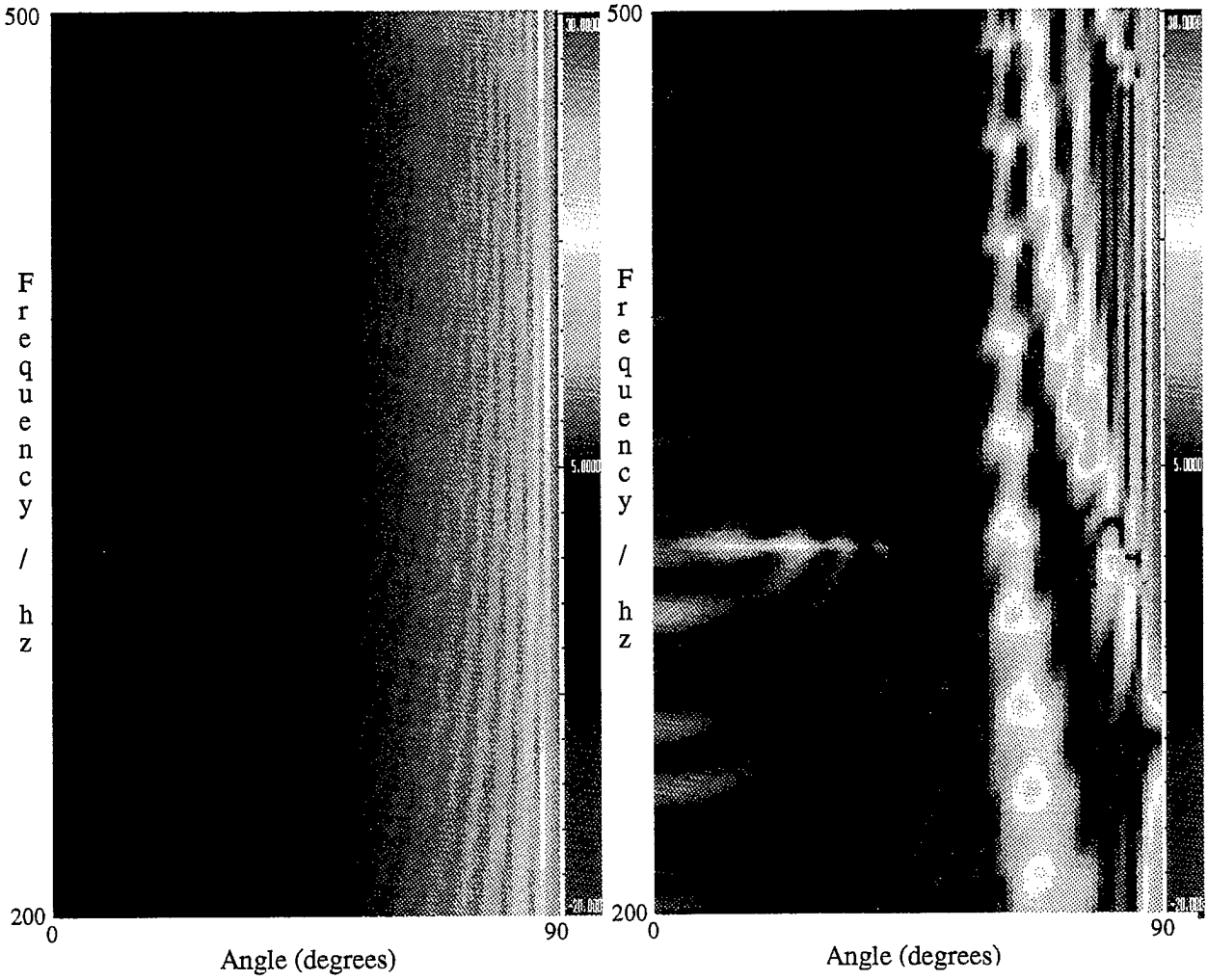

FIG. 5. Monostatic target strength using (a) the TAP model and (b) Sara–2d computations.

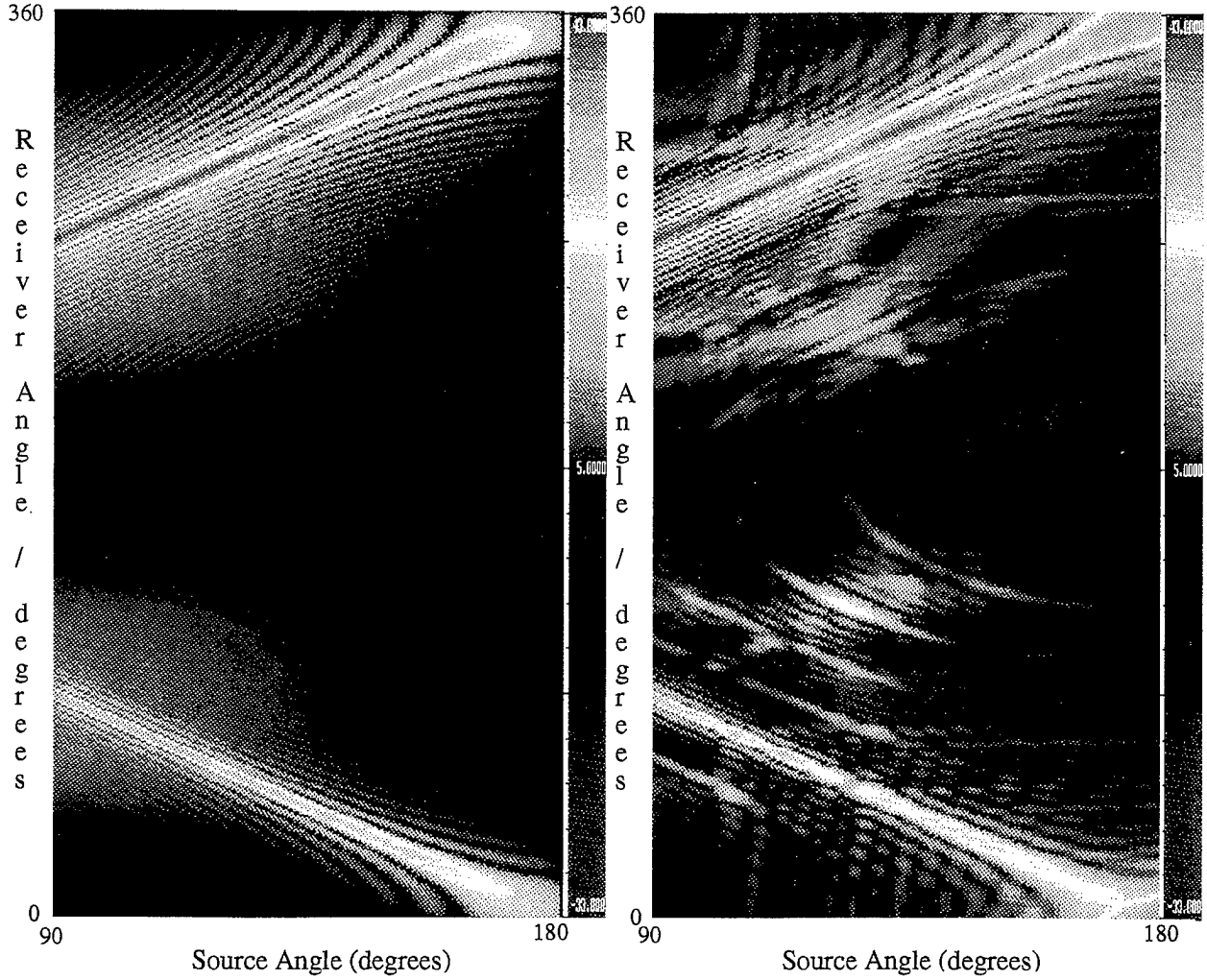

(a) (b)

FIG. 6. Target strength at a frequency of 700Hz, ka=9.00, using (a) the TAP model and (b) Sara–2d computations with a ribbed cylinder.

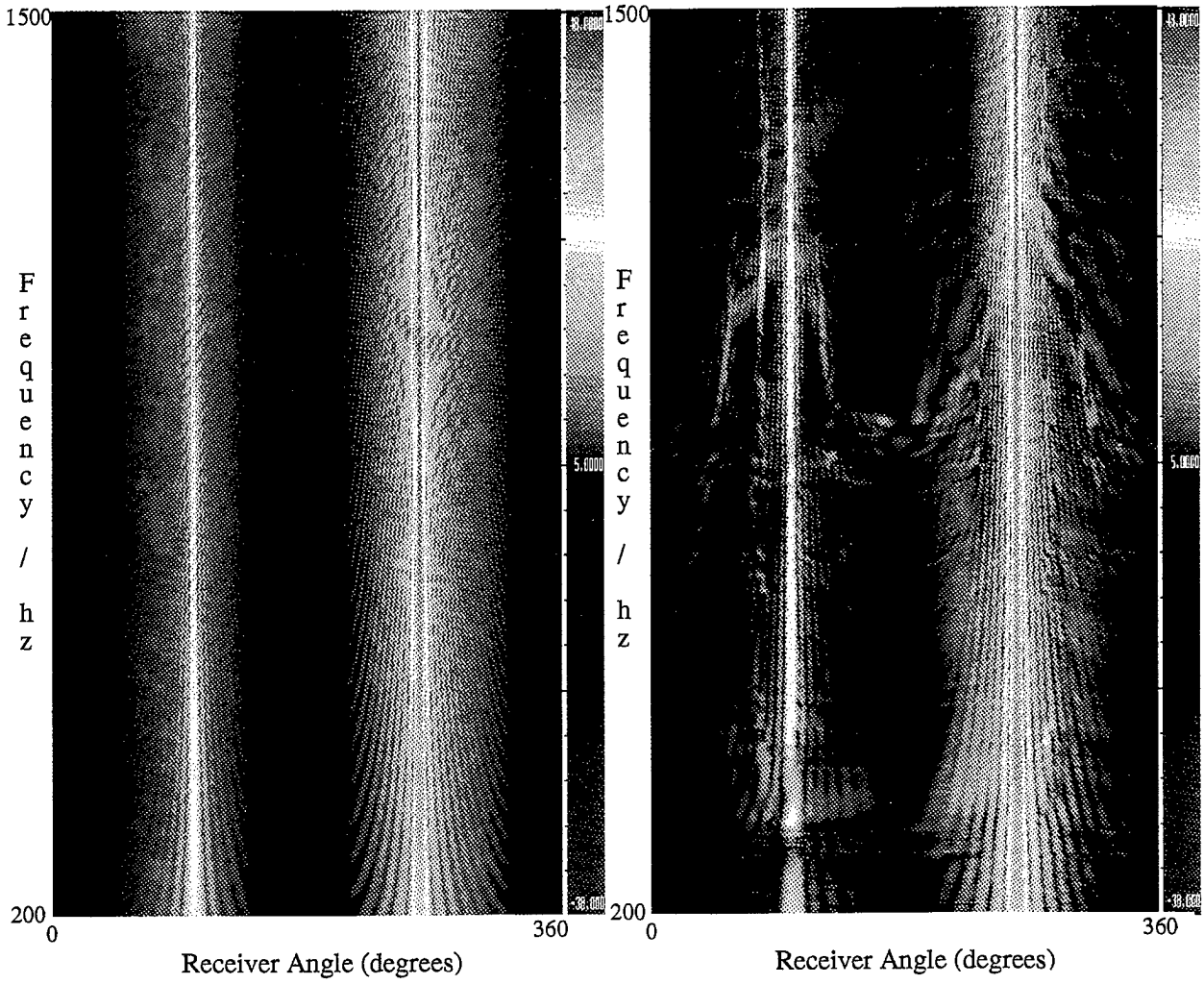

FIG. 7. Bistatic target strength for a source angle of 80 degrees using (a) the TAP model and (b) Sara–2d computations with a ribbed cylinder.

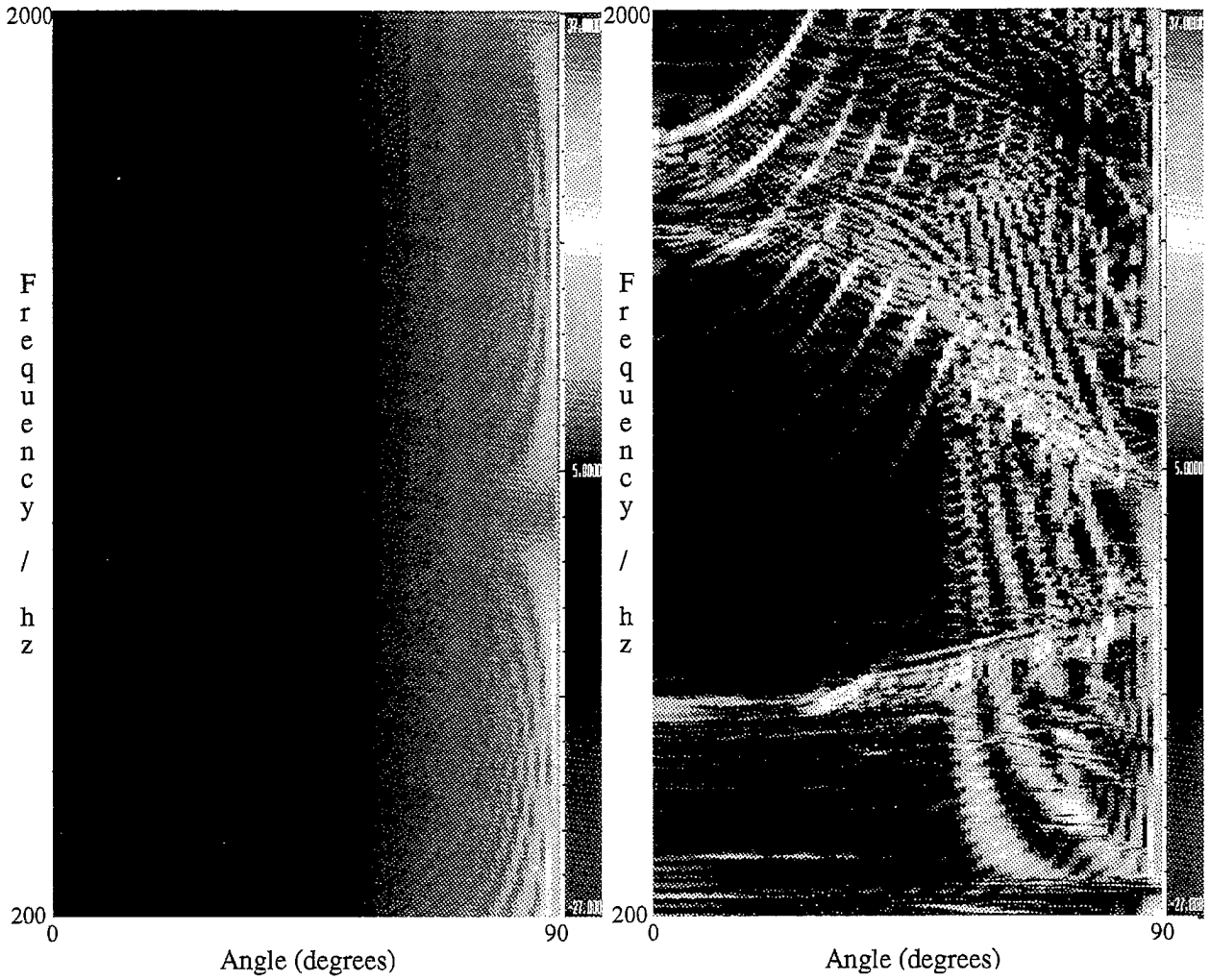

FIG. 8. Monostatic target strength using (a) the TAP model and (b) Sara–2d computations with a ribbed cylinder.

[2]H. Allik, R. Dees, S. Moore and D. Pan, "Sara-2d User's Manual," version 95-3, BBN Systems and Technologies, New London, Connecticut (1995).

[3]O. C. Zienkiewicz, C. Emson and P. Bettess, "A Novel Boundary Infinite Element," Int. J. Num. Meth. Engng., **19**, 393-404(1983).

[4]O. C. Zienkiewicz, K. Bando, P. Bettess, C. Emson and T. C. Chiam, "Mapped Infinite Elements for Exterior Wave Problems," Int. J. Num. Meth. Engng., **21** 1229-1251(1985).

[5]M. Born and E. Wolf, *Principles of Optics*, p. 381 Fifth ed. (Pergamon Press, Oxford, 1975).